
Volume 21 Number 5 July 2007
ISSN 0888 – 3270
ELSEVIER
mssp
Mechanical Systems & Signal Processing
Diagnostics
Modal analysis
Measurements / Modeling / Control
Vibration / Noise
Available online at
ScienceDirect
www.sciencedirect.com

Available online at www.sciencedirect.com
ScienceDirect
Mechanical Systems and Signal Processing 21 (2007) 2125–2136
Mechanical Systems and Signal Processing
www.elsevier.com/locate/jnlabr/ymssp

Estimation of modal parameters using bilinear joint time–frequency distributions

A. Roshan-Ghias[a], M.B. Shamsollahi[b,*,1], M. Mobed[b], M. Behzad[a]

[a] Mechanical Engineering Department, Sharif University of Technology, Tehran, Iran
[b] Electrical Engineering Department, Sharif University of Technology, Tehran, Iran

Received 15 March 2006; received in revised form 24 July 2006; accepted 29 September 2006
Available online 1 December 2006

Abstract

In this paper, a new method is proposed for modal parameter estimation using time–frequency representations. Smoothed Pseudo Wigner–Ville distribution which is a member of the Cohen's class distributions is used to decouple vibration modes completely in order to study each mode separately. This distribution reduces cross-terms which are troublesome in Wigner–Ville distribution and retains the resolution as well. The method was applied to highly damped systems, and results were superior to those obtained via other conventional methods.

Keywords: Modal parameter estimation; Joint time–frequency distributions; Highly damped systems

1. Introduction

Numerous algorithms have been developed for estimating modal parameters using time and frequency domains separately over the past 30 years. In recent years, joint time–frequency (JTF) and wavelet transform (WT) methods have attracted many researchers to use great capabilities of these transforms.

Several papers have been published on applying WT for estimating modal parameters in recent years. Lardies and Gouttebroze [1] used WT and presented a special form of the Morlet Wavelet which gave rewarding results. Le and Argoul [2] studied three different wavelets and tackled the "Edge Effect" problem. Haase and Widjajakusuma [3] presented a method based on the WT for fault detection using modal parameters. On the other hand, there are researches in Biomedical Magnetic Resonance Spectroscopy which are very similar to the modal analysis. Serrai et al. [4] used the Morlet Wavelet and established an algorithm with less approximation in comparison with some other works.

However, to the best of the authors' knowledge, no work has yet been reported on estimating modal parameters using bilinear JTF distributions. These distributions expand the energy of a signal concurrently in

*Corresponding author. Tel.: +98 21 6616 4356.
E-mail address: mbshams@sharif.edu (M.B. Shamsollahi).
[1]Postal address: Electrical Engineering Department – Sharif University of Technology – Azadi street – Tehran – Iran.

0888-3270/$ - see front matter
doi:10.1016/j.ymssp.2006.09.009

time and frequency. This makes them a natural choice for fully decoupling the modes of vibration which happen at distinct frequencies.

Wigner–ville distribution (WVD) which is a member of Cohen's class distributions has the best resolution in time–frequency plane among all time–frequency representations of this class. But it has a deficiency of so-called cross-terms. Cross-terms appear when a signal has two or more components in the time–frequency plane. In a free decay response signal, these components are different modes of vibration. Thus, WVD is incapable of giving an appropriate discrimination of these components in the time–frequency plane in general. In order to compensate this drawback, dozens of joint time–frequency representations have been introduced during last decades [5–8].

Smoothed Pseudo Wigner–Ville (SPWV) is a member of Cohen's class distributions which utilizes two different smoothing windows on WVD, separately in time and in frequency, and eliminates cross-terms considerably [6].

In this paper, we introduce a method for the estimation of modal parameters using the SPWV distribution. Free decay response of a linear mechanical system with proportional damping ratios is used to estimate modal parameters (natural frequency and damping) of the system. It can be applied to single-degree-of-freedom (sdof) and multi-degree-of-freedom (mdof) linear systems. The exact analytical time-frequency distribution of a one-dof system is obtained and modal parameters are extracted from the formulation. Afterward, in view of the fact that SPWV decouples vibration modes in the time-frequency domain, results are expanded to a mdof system. In order to demonstrate the capability of the proposed method, the damping ratio estimation of a 2dof highly damped system is examined and compared to two other methods.

The paper is organized as follows. Section 2 is a brief introduction to Cohen's class distributions and SPWV characteristics. In Section 3, WVD of the free decay response of a sdof system is obtained. The SPWV of free decay response of a sdof system is derived in Section 4. Section 5 generalizes the results of the sdof system to mdof systems considering the fully decoupling of vibration modes in time–frequency domain. In Section 6, two examples are given and fully discussed. Finally concluding remarks are given in Section 7.

2. Cohen's class

The representations that describe a signal's frequency behavior fall predominantly into two categories [5]: linear representations such as the Fourier transform, and quadratic representations such as the power spectrum (PS). Quadratic representations can be viewed as distributing signal's energy into frequency, time–frequency, or time-scale variables. In this section we introduce a counterpart to the power spectrum: the quadratic joint time frequency representation known as Cohen's class distributions. The main core of all TFR is the Wigner–Ville Distribution (WVD) which is defined as:

$$\mathrm{WVD}_x(t,f) = \int_{-\infty}^{\infty} x\left(t+\tau/2\right)x^*\left(t-\tau/2\right)\mathrm{e}^{-j2\pi f\tau}\,\mathrm{d}\tau. \tag{1}$$

WVD can be seen as the instantaneous version of the power spectrum [6]. Theoretically, the WVD has the best time–frequency resolution among all time-frequency representations. But it does suffer from the serious problem of cross-terms, which occurs when the signal has two or more distinct time–frequency features [7].

In order to overcome this deficiency, other bilinear JTF distributions have been developed over the last decades such as the Pseudo WVD (PWVD), Smoothed Pseudo WVD (SPWVD) [6], Choi-Williams distribution (CWD) and cone-shape distribution (ZAMD) [5]. It is interesting to note that all these bilinear representations can be written in a general form that was introduced by Cohen [5]. The discovery of the general form of bilinear TFR facilitates us with the design of the desired TFR.

This general form can be written as

$$\begin{aligned} T_x(t,f) &= \int_{-\infty}^{\infty}\int_{-\infty}^{\infty}\int_{-\infty}^{\infty} \Phi(t-s,f-\eta)x\left(s+\frac{\tau}{2}\right)x^*\left(s-\frac{\tau}{2}\right)\mathrm{e}^{-j2\pi\eta\tau}\,\mathrm{d}\tau\,\mathrm{d}s\,\mathrm{d}\eta \\ &= \int_{-\infty}^{\infty}\int_{-\infty}^{\infty} \Phi(t-s,f-\eta)WVD_x(s,\eta)\,\mathrm{d}s\,\mathrm{d}\eta, \end{aligned} \tag{2}$$

where $\Phi(t, f)$ is a two dimensional filter known as *the kernel of the* TFR. It can be seen that when $\Phi(t,f) = \delta(t)\delta(f)$, WVD is obtained. Sometimes it is more convenient to use $\varphi(\tau, \upsilon)$ instead, which is the inverse 2-D Fourier transform of $\Phi(t, f)$ [5].

Smoothed pseudo Wigner–Ville is a member of Cohen's class with a separable kernel in the form:

$$\Phi(t,f) = g(t)H(f) \quad \text{or} \quad \varphi(\tau, v) = h(\tau)G(v). \tag{3}$$

This characteristic enables us to determine each window separately to suit our requirements. Windowing reduces cross-terms considerably but at the cost of losing some resolution.

3. Application of WVD to free decay response of sdof systems

Consider a sdof mechanical system with viscous damping ξ_0. The free displacement response (noise free) according to modal basis is expressed as

$$x(t) = \Phi_0\, e^{-2\pi\xi_0 f_0 t} \cos(2\pi\bar{f}_0 t + \varphi_0)u(t), \tag{4}$$

where f_0 and $\bar{f}_0$ are the undamped and damped natural frequencies in Hz, Φ_0 is the amplitude of vibration and $u(t)$ is the Heaviside function. If $x(t)$ is assumed asymptotic, that is if the phase of the signal varies much faster than the amplitude (which implies that $\xi_0 \ll 1/\sqrt{2}$), it can be shown [2] that the complex signal

$$x_a(t) = \Phi_0\, e^{-2\pi\xi_0 f_0 t}\, e^{j(2\pi\bar{f}_0 t + \varphi_0)} u(t), \tag{5}$$

is a good approximation of the analytic signal. Analytic signal is more appropriate to use since the WVD of the analytical signal has less cross-terms than the WVD of the real signal [5], so Eq. (5) is used instead of Eq. (4).

Using Eq. (1), the WVD of free decay response can be expressed as (see Appendix A)

$$WVD_x(t,f) = \frac{\Phi_0^2\, e^{-4\pi f_0 \xi_0 t}}{4\pi(f - \bar{f}_0)} \sin 4\pi(f - \bar{f}_0)t. \tag{6}$$

Although at $f = \bar{f}_0$, this function is undefined but its limit is

$$\lim_{f \to \bar{f}_0} WVD_x(t,f) = \Phi_0^2 t\, e^{-4\pi f_0 \xi_0 t}. \tag{7}$$

Fig. 1(a) shows a typical WVD of a free decay response and Fig. 1(b) shows its value at the damped natural frequency. As it is seen in Fig. 1(a) and in Eq. (6), at the damped natural frequency, this function has a maximum. Thus $\bar{f}_0$ and the corresponding slice of the time–frequency map can be easily obtained without any

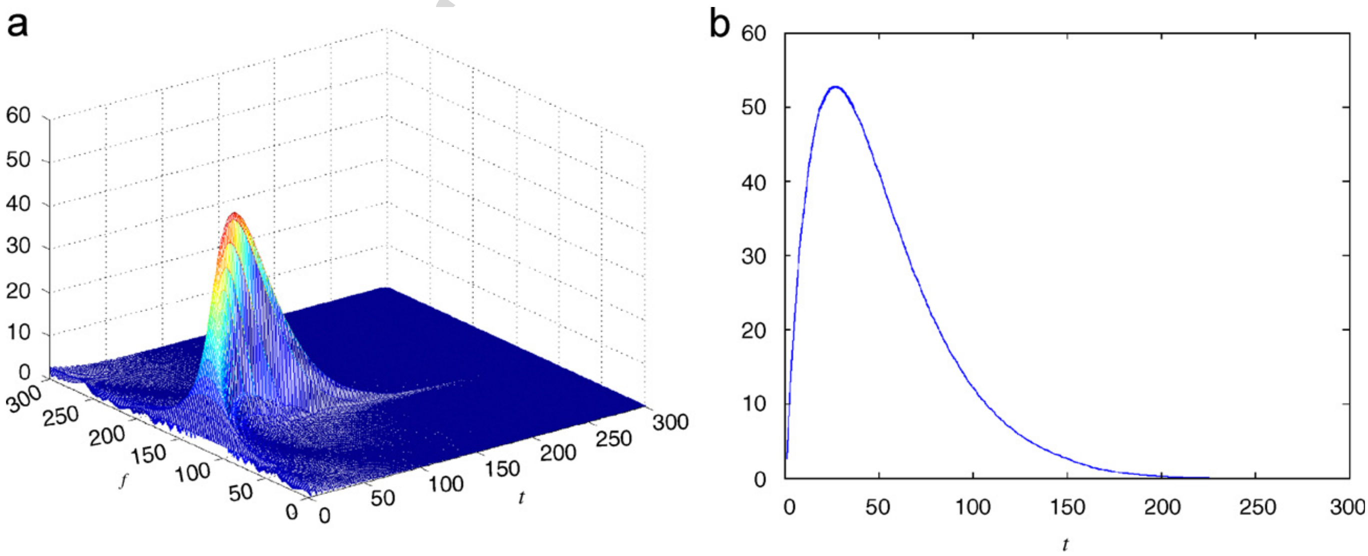

Fig. 1. (a) WVD of a typical free decay response, and (b) WVD value at the damped natural frequency.

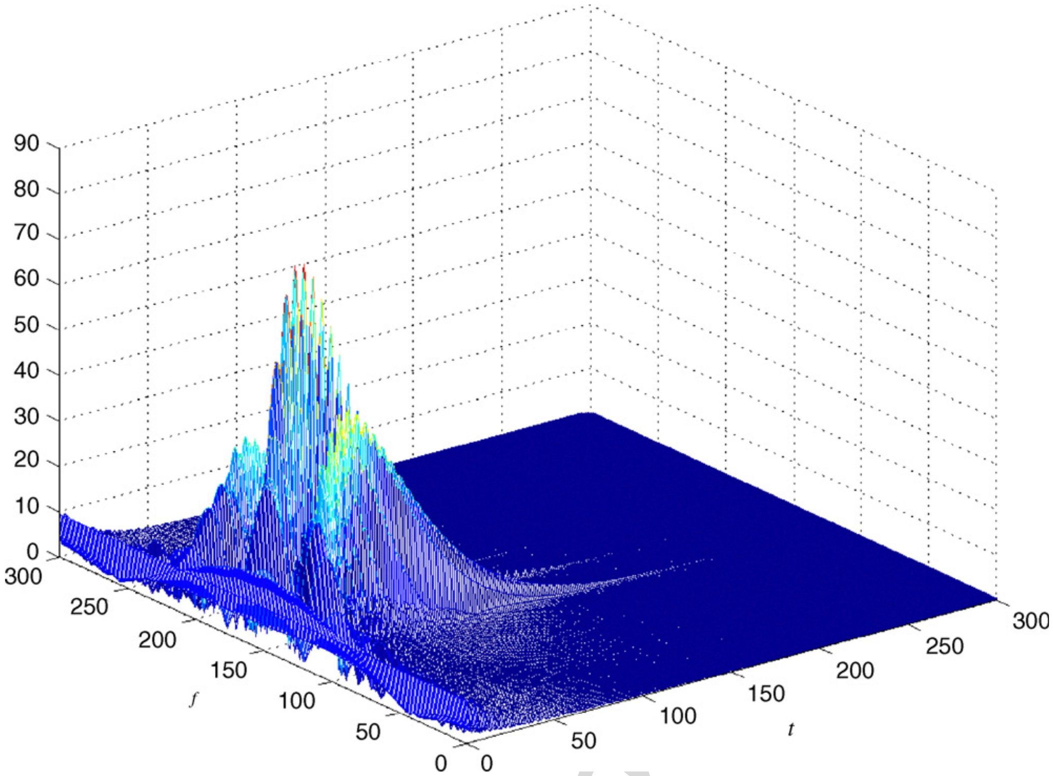

Fig. 2. WVD of a typical free decay response of a two degrees of freedom system.

computations. Then using Eq. (7) and a simple curve fitting algorithm, ξ_0 can be calculated (the very beginning and the very end of the calculated WVD at the damped natural frequency should be omitted to avoid errors due to the edge-effect problem).

For any sdof system, this method is accurate and the cost of computation is low. But in the case of mdof systems, this method fails to give reasonable results because of the above-mentioned cross-terms (Fig. 2).

4. Application of SPWVD to free decay response of sdof systems

As it was stated before, knowing WVD of a signal, its SPWV distribution can be written as

$$SPWV_x(t,f) = \int_{-\infty}^{\infty}\int_{-\infty}^{\infty} WVD_x(t-s, f-\eta)g(s)H(\eta)\,\mathrm{d}s\,\mathrm{d}\eta. \tag{8}$$

Looking at the WVD of a mdof free decay response reveals the nature of the cross-terms. Since every mode has a fixed frequency in the time-frequency plane, cross-terms occur at the middle of every two of them. In other words, cross-terms are at fixed frequencies too. It can be proved [5] that in this case, there is no need of the frequency smoothing window. So the function H in the kernel of SPWVD will be set to Kronecker delta function. The resulting representation is the counterpart to Pseudo Wigner-Ville Distribution which has only the frequency smoothing window. Therefore Eq. (8) can be simplified to

$$SPWV_x(t,f) = \int_{-\infty}^{\infty} WVD_x(t-s, f)g(s)\,\mathrm{d}s. \tag{9}$$

The Gaussian window is an appropriate candidate for the time smoothing window since it is a low-pass filter with the analytical form of

$$g(t) = \frac{1}{\sqrt{2\pi}\sigma}\,\mathrm{e}^{-t^2/2\sigma^2}, \tag{10}$$

where σ is the windowing parameter.

Substituting Eqs. (6) and (10) into Eq. (9), we get integrals of the form:

$$\begin{aligned} SPWV_x(t,f) &= A_1\sigma\int_{-t/\sigma}^{\infty}\exp\left\{-\frac{u^2}{2}+\sigma\left[-4\pi\xi_0 f_0+j4\pi(f-\bar{f}_0)\right]u\right\}\mathrm{d}u \\ &\quad - A_2\sigma\int_{-t/\sigma}^{\infty}\exp\left\{-\frac{u^2}{2}-\sigma\left[-4\pi\xi_0 f_0+j4\pi(f-\bar{f}_0)\right]u\right\}\mathrm{d}u, \end{aligned} \tag{11}$$

where

$$\begin{aligned} A_1 &= \frac{\Phi_0^2}{\sqrt{2\pi}\sigma}\times\frac{1}{j4\pi(f-\bar{f}_0)}\times\exp\left\{-4\pi\xi_0 f_0 t+j4\pi(f-\bar{f}_0)t\right\} \\ A_2 &= \frac{\Phi_0^2}{\sqrt{2\pi}\sigma}\times\frac{1}{j4\pi(f-\bar{f}_0)}\times\exp\left\{-4\pi\xi_0 f_0 t-j4\pi(f-\bar{f}_0)t\right\}. \end{aligned} \tag{12}$$

Using substitute variables a_1, a_2, Δ_1, Δ_2 and α, Eq. (11) can be written as

$$SPWV_x(t,f) = A_1\sigma\,\mathrm{e}^{a_1^2/2+ja_1\Delta_1}I_1 - A_2\sigma\,\mathrm{e}^{a_2^2/2+ja_2\Delta_2}I_2, \tag{13}$$

where

$$I_1=\int_{\alpha}^{\infty}\mathrm{e}^{-t^2/2+j\Delta_1 t}\,\mathrm{d}t,\quad I_2=\int_{\alpha}^{\infty}\mathrm{e}^{-t^2/2+j\Delta_2 t}\,\mathrm{d}t, \tag{14}$$

$$\alpha = t/\sigma-4\pi\xi_0 f_0\sigma,\quad a=a_1=a_2=-4\pi\xi_0 f_0\sigma,\quad \Delta=\Delta_1=-\Delta_2=4\pi(f-\bar{f}_0)\sigma. \tag{15}$$

Integrals of Eq. (14) do not have primary functions, but they can be obtained with desired accuracy (see Appendix B). Substituting integral's value, we can write Eq. (13) as

$$SPWV_x(t,f) = Y\left\{B\sin\left[4\pi(f-\bar{f}_0)\alpha\right]+C\cos\left[4\pi(f-\bar{f}_0)\alpha\right]\right\}, \tag{16}$$

where

$$Y=\frac{\Phi_0^2}{\sqrt{2\pi}}\times\frac{1}{2\pi(f-\bar{f}_0)}\times\exp\left\{-4\pi\xi_0 f_0 t+(4\pi\xi_0 f_0)^2/2\right\}, \tag{17}$$

$$B=\sqrt{\frac{\pi}{2}}\left(\mathrm{e}^{-\Delta^2/2}\mp\sqrt{1-\mathrm{e}^{-\alpha^2}}\right), \tag{18}$$

$$C=\pm\sqrt{\frac{\pi}{2}}\mathrm{e}^{-\Delta^2/2}\left(\sqrt{\mathrm{e}^{\Delta^2}-1}\right)-\Delta\left(1-\mathrm{e}^{-\alpha^2/2}\right). \tag{19}$$

The signs $\mp$ in Eq. (18) and $\pm$ in Eq. (19) are conditioned by the signs of α and Δ, respectively.

Obviously, Eqs. (16)–(19) are complicated. However, similar to the WVD case, the expressions simplify when $f\to\bar{f}_0$:

$$\lim_{f\to\bar{f}_0} SPWV_x(t,f)=\Phi_0^2\sigma\mathrm{e}^{-4\pi f_0\xi_0\sigma\left[\alpha+\frac{1}{2}4\pi f_0\xi_0\sigma\right]}\left\{\alpha+\alpha\times erf\left(\frac{\alpha}{\sqrt{2}}\right)+\sqrt{\frac{2}{\pi}}\mathrm{e}^{-\frac{1}{2}\alpha^2}\right\}, \tag{20}$$

where

$$erf(x)=\frac{2}{\sqrt{\pi}}\int_0^x \mathrm{e}^{-t^2}\,\mathrm{d}t, \tag{21}$$

and finally using the same procedure as in the WVD case, Eq. (21) can be used to find Φ_0 and ξ_0.

5. Application of SPWVD to free decay response of mdof systems

In the case of mdof systems, free decay response can be expressed as the sum of all modes:

$$x_m(t) = \sum_{k=1}^{N} \Phi_{mk}\, \mathrm{e}^{-2\pi\xi_k f_k t} \cos(2\pi \bar{f}_k t + \varphi_k) u(t), \tag{22}$$

where k is the mode number. Assuming the signal to be asymptotic (all $\xi_k \ll 1/\sqrt{2}$), the analytic form can be written as

$$x_{m_a}(t) = \sum_{k=1}^{n} \Phi_{mk}\, \mathrm{e}^{-2\pi\xi_k f_k t}\, \mathrm{e}^{j(2\pi \bar{f}_k t + \varphi_k)} u(t). \tag{23}$$

Assuming the cross-terms to be negligible (because of the implication of the time smoothing window, the cross-terms would be reduced significantly), the SPWVD of Eq. (23) can be written as

$$SPWV_x(t,f) = \sum_{k=1}^{N} Y_k \{ B_k \sin[4\pi(f - \bar{f}_k)\alpha_k] + C_k \cos[4\pi(f - \bar{f}_k)\alpha_k] \}. \tag{24}$$

Similar to the sdof case, the SPWV distribution is maximum at damped natural frequencies. Hence using a peak-picking algorithm, the damped natural frequency of each mode can be estimated. Subsequently, a curve-fitting algorithm with corresponding slices of the time–frequency map and Eq. (20) will yield the damping ratio of each mode.

6. Simulated results

In order to demonstrate the capability of the SPWVD based method in modal analysis, a simulation is done with a two-dof system. The parameters of the system are given in Table 1. The free decay response and the frequency response of this system are shown in Fig. 3. The SPWVD of this signal is shown in Fig. 4(a), (b) and the ridges which correspond to damped natural frequencies are given in Figs. 4(c), (d). Using the procedure described in Section 5, the natural frequencies and damping ratios of the two modes is extracted (Table 2). In this case, the accuracy of the SPWV based method is the same as two other methods: Line-fit method (LFM) and rational fraction polynomial method (RFPM) [9].

However in some special cases, such as in highly damped systems, this method shows a great improvement with respect to other methods. Consider a 2dof system with initial modal parameters which is shown in Table 3. Damping ratios in both modes were increased stepwise up to 15% and then the modal parameters were estimated using SPWV and other methods. Estimated natural frequencies were satisfactory in all methods, but estimating high dampings becomes inaccurate Table 4. Figs. 5 and 6 show the percentage of error for both modes in each method, when damping is increased. The accuracy of the SPWV based method is undoubtedly higher than those two other methods. This is due to the perfect decoupling of the modes in the time-frequency domain using the SPWV distribution.

7. Conclusion

A novel method in modal parameter identification using smoothed pseudo Wigner–Ville distribution was proposed. Time-frequency representations fully decouple vibration modes and it makes them an enhanced tool

Table 1
Modal parameters of a 2dof system

	Frequency (Hz)	Damping (%)
1st mode	10	2.5
2nd mode	35	1

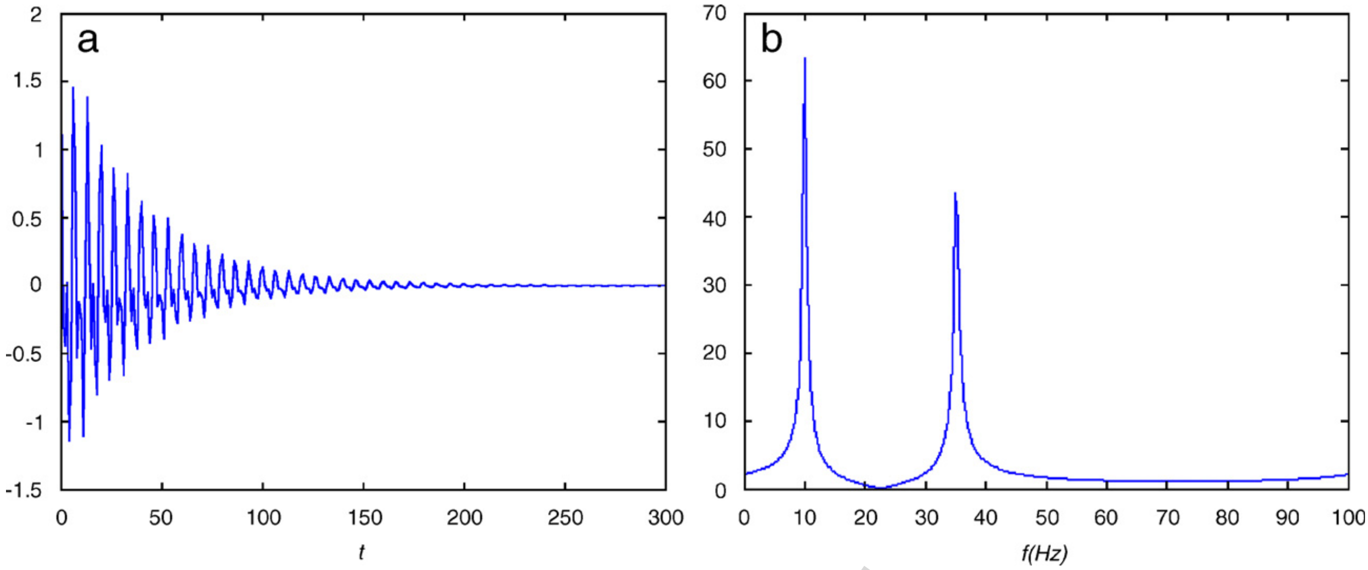

Fig. 3. (a) Time response of a 2dof system, and (b) frequency response of a 2dof system.

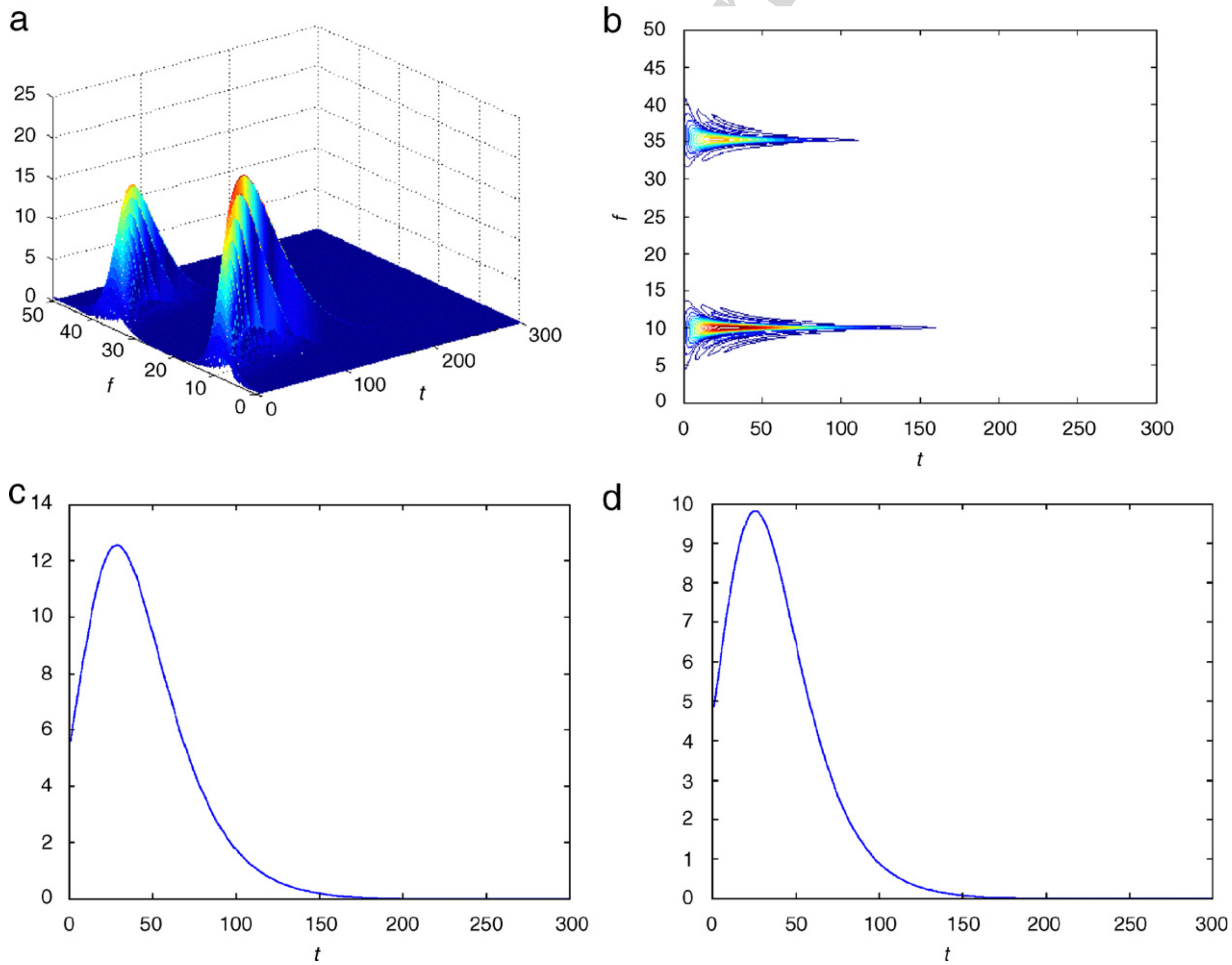

Fig. 4. (a,b) SPWVD of a 2dof system, (c) ridge plot at the first natural frequency, and (d) ridge plot at the second natural frequency.

Table 2
Estimated modal parameters for the first mode

	Frequency (Hz)	Damping (%)
SPWVD	10.00	2.52
LFM	10.00	2.51
RPFM	10.00	2.51

Table 3
Modal parameters of a 2dof system

	Frequency (Hz)	Damping (%)
1st mode	20	2.5
2nd mode	35	2.5

Table 4
Exact and estimated values of damping ratios

Damping ratio of 1st mode (%)				Damping ratio of 2nd mode (%)			
Exact	LFM	RFPM	SPWV	Exact	LFM	RFPM	SPWV
2.5	2.5593	2.5123	2.51	2.5	2.4776	2.5145	2.48
5	5.2379	4.9115	4.93	5	4.8197	5.085	4.91
7.5	7.7719	7.4312	7.67	7.5	7.046	7.4443	7.32
10	10.6616	9.8489	10.05	10	9.3642	10.3476	9.97
12.5	13.4623	12.2601	12.42	12.5	11.2924	12.8336	12.47
15	16.5267	14.5118	14.94	15	13.1857	14.778	14.96

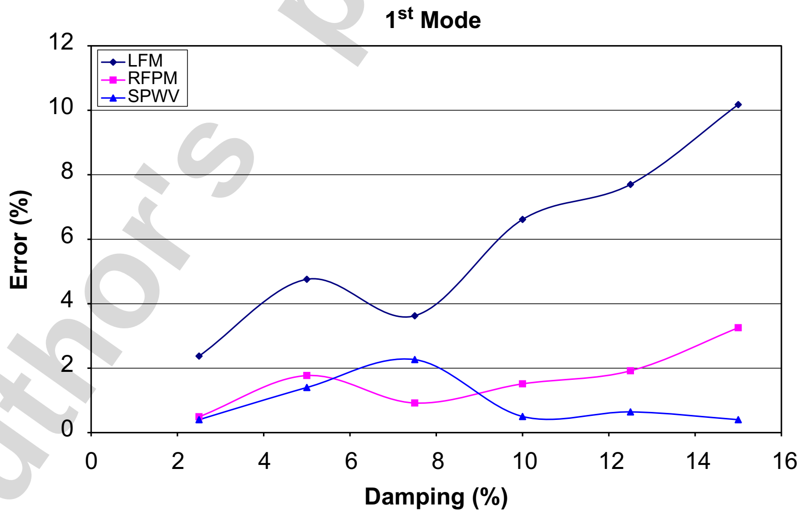

Fig. 5. Amount of error in estimating damping of the first mode.

in modal analysis. Because of this decoupling, each natural frequency can be obtained with a simple pick-peaking algorithm along the frequency axis. An analytic form of a free decay response of a sdof system was obtained in the time–frequency plane using SPWVD, without any simplifying approximation. Therefore modal damping can be obtained with a straightforward curve-fitting for each mode. The method shows its effectiveness in modal analysis of highly damped systems where most other methods encounter large errors.

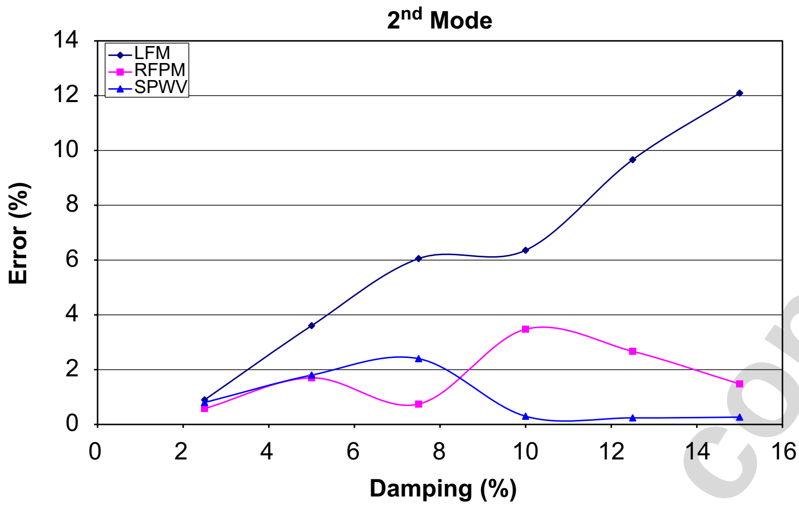

Fig. 6. Amount of error in estimating damping of the second mode.

Appendix A

This appendix describes the calculation of the Wigner–Ville distribution of the free decay response of a sdof system. Substituting Eq. (5) into Eq. (1) yields

$$\begin{aligned} WV_x(t,f) = \frac{1}{4}\int_{-\infty}^{\infty} \Phi_0\, \mathrm{e}^{-2\pi\xi_0 f_0(t+\tau/2)}\, \mathrm{e}^{j[2\pi\bar{f}_0(t+\tau/2)+\varphi_0]} u(t+\tau/2) \\ \times\, \Phi_0\, \mathrm{e}^{-2\pi\xi_0 f_0(t-\tau/2)}\, \mathrm{e}^{-j[2\pi\bar{f}_0(t-\tau/2)+\varphi_0]} u(t-\tau/2)\, \mathrm{e}^{-j2\pi f\tau}\, \mathrm{d}\tau, \end{aligned} \tag{A.1}$$

which is simplified to

$$WV_x(t,f) = \frac{1}{4}\Phi_0^2 \mathrm{e}^{-4\pi\xi_0 f_0 t}\int_{-2t}^{2t} \mathrm{e}^{-j2\pi(f-\bar{f}_0)\tau}\, \mathrm{d}\tau = \frac{\Phi_0^2\, \mathrm{e}^{-4\pi\xi_0 f_0 t}}{j8\pi(f-\bar{f}_0)}\left[\mathrm{e}^{j2\pi(f-\bar{f}_0)\tau}\right]_{\tau=-2t}^{2t}, \tag{A.2}$$

and finally

$$WV_x(t,f) = \frac{\Phi_0^2\, \mathrm{e}^{-4\pi\xi_0 f_0 t}}{4\pi(f-\bar{f}_0)} \sin\left(4\pi(f-\bar{f}_0)t\right). \tag{A.3}$$

Appendix B

This appendix provides the computation of the integral $I = \int_{\alpha}^{\infty} \mathrm{e}^{[(-\tau^2/2)+j\Delta\tau]}\, \mathrm{d}\tau$, where $\alpha = t/\sigma - 4\pi\xi_0 f_0 \sigma$ [4]. I may be written as

$$\begin{aligned} I &= \int_0^{\infty} \mathrm{e}^{[(-\tau^2/2)+j\Delta\tau]}\, \mathrm{d}\tau - \int_0^{\alpha} \mathrm{e}^{[(-\tau^2/2)+j\Delta\tau]}\, \mathrm{d}\tau \\ &= I_1 - I_2 \quad \forall\alpha. \end{aligned} \tag{B.1}$$

Consider the rectangle OABC in Fig. 7. Let $f(z)$ be a complex function on this rectangle, given by $f(z) = \mathrm{e}^{-z^2/2}$, where $z = \tau - j\Delta$ and t runs from 0 to ∞. I_1 may be written as

$$I_1 = \mathrm{e}^{-\Delta^2/2}\int_{-j\Delta}^{\infty - j\Delta} \mathrm{e}^{-z^2/2}\, \mathrm{d}z. \tag{B.2}$$

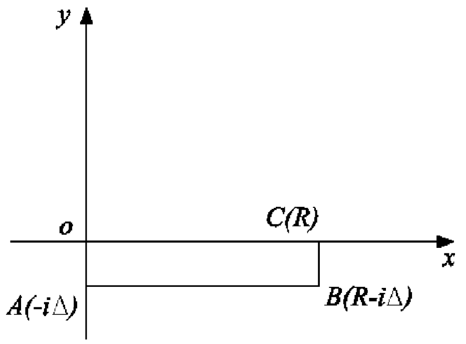

Fig. 7. A rectangle in complex plane.

The function $e^{-z^2/2}$ is analytical on and inside the rectangle OABCO. Using Cauchy theorem, we have

$$\oint_{OABCO} f(z)\,dz = \int_{OA} e^{-z^2/2}\,dz + \int_{AB} e^{-z^2/2}\,dz + \int_{BC} e^{-z^2/2}\,dz + \int_{CO} e^{-z^2/2}\,dz = 0. \tag{B.3}$$

(1) On the segment OA of the rectangle, $z = -jy$, where y runs from 0 to Δ. Using the polar coordinate ($r \in [0, \sqrt{2}\Delta]$, $\theta \in [0, \pi/2]$) and the sign of Δ, $f(z)$ is given by

$$\int_{OA} e^{-z^2/2}\,dz = \int_0^{\infty} -je^{y^2/2}\,dy \approx \mp j\left[\frac{\pi}{2}(e^{\Delta^2} - 1)\right]^{1/2}. \tag{B.4}$$

(2) On the segment AB of the rectangle, $z = x - j\Delta$, $x \in [0, R]$, so that

$$\int_{AB} e^{-z^2/2}\,dz = \int_{-j\Delta}^{R-j\Delta} e^{-(x-j\Delta)^2/2}\,dx. \tag{B.5}$$

Eq. () is I_1 up to the term $e^{-\Delta^2/2}$.

(3) On the segment BC of the rectangle, $z = R - jy$, $y \in [\Delta, 0]$. Thus,

$$\int_{BC} e^{-z^2/2}\,dz = -j\int_{\Delta}^{0} e^{-(R-jy)^2/2}\,dy = -je^{-R^2/2}\int_{\Delta}^{0} e^{(jRy+y^2/2)}\,dy. \tag{B.6}$$

Eq. (B.6) may be estimated in the limit by

$$\int_{BC} e^{-z^2/2}\,dz \leqslant -je^{-R^2/2}\int_{\Delta}^{0} e^{y^2/2}\,dy. \tag{B.7}$$

The integral $\int_{\Delta}^{0} e^{y^2/2}\,dy$ has a finite value; hence, Eq. (B.7) decreases to zero when $R \to \infty$.

(4) On segment CO, $z = x$, with $x \in [R, 0]$ Using the polar coordinates ($r \in [0, \sqrt{2}\Delta], \theta \in [0, \pi/2]$), we obtain

$$\int_{CO} e^{-z^2/2}\,dz = -\int_0^{R} e^{-x^2/2}\,dy \approx -\left[\sqrt{\frac{\pi}{2}}\left(1 - e^{-R^2}\right)\right]^{1/2}, \tag{B.8}$$

Eq. (B.8) approaches $-\sqrt{\pi/2}$ when $R \to \infty$.

Substituting the values of Eqs. (B.4)–(B.7) into Eq. (B.8), we obtain

$$I_1 \approx \begin{cases} \sqrt{\frac{\pi}{2}}e^{-\Delta^2/2}\left[1 + j\sqrt{e^{\Delta^2} - 1}\right] & \text{if } \Delta > 0, \\ \sqrt{\frac{\pi}{2}}e^{-\Delta^2/2}\left[1 - j\sqrt{e^{\Delta^2} - 1}\right] & \text{if } \Delta < 0. \end{cases} \tag{B.9}$$

For $I_2 = \int_0^\alpha e^{t^2/2} e^{j\Delta t}\, dt$, we use the Taylor series expansion of the term $e^{j\Delta}$.

$$I_2 = \int_0^\alpha \left[\sum_{k=0}^{\infty} \frac{(j\Delta t)^k}{k!} \right] e^{-t^2/2}\, dt = \sum_{k=0}^{\infty} \frac{(j\Delta)^k}{k!} \int_0^\alpha t^k e^{-t^2/2}\, dt = \sum_{k=0}^{\infty} \frac{(j\Delta)^k}{k!} U_k, \tag{B.10}$$

where $U_k = \int_0^\alpha t^k e^{-t^2/2}\, dt$. If $k = 0$ and the polar coordinates are used:

$$U_0 = \int_0^\alpha e^{-t^2/2}\, dt \approx \begin{cases} \sqrt{\frac{\pi}{2}}\sqrt{1 - e^{-\alpha^2}} & \text{if } \alpha > 0 \\ -\sqrt{\frac{\pi}{2}}\sqrt{1 - e^{-\alpha^2}} & \text{if } \alpha > 0. \end{cases} \tag{B.11}$$

If $k = 1$, by changing variables, we obtain $U_1 = \int_0^\alpha t e^{-t^2/2}\, dt = \left[1 - e^{-\alpha^2/2}\right]$. The general term for this series for $k \geqslant 2$, is given by

$$\begin{aligned} U_k &= \int_0^\alpha t^k e^{-t^2/2}\, dt = -\int_0^\alpha t^{k-1} (e^{-t^2/2})'\, dt \\ &= -\alpha^{k-1} e^{-\alpha^2/2} + (k-1) \int_0^\alpha t^{k-2} e^{-t^2/2}\, dt = -\alpha^{k-1} e^{-\alpha^2/2} + (k-1) U_{k-2}. \end{aligned} \tag{B.12}$$

The series $\sum_{k=0}^{\infty} \left[(j\Delta)^k / k!\right] U_k$ is recurrent and convergent.

By combining Eqs. (B.1), (B.9) and (B.10), I is approximated as

$$I \approx \left[\sqrt{\frac{\pi}{2}} e^{-\Delta^2/2} \left(1 \pm j\sqrt{e^{\Delta^2} - 1} \right) \right] - \sum_{k=0}^{\infty} \left[\frac{(j\Delta)^k}{k!} \right] U_k \quad \forall \alpha. \tag{B.13}$$

Eq. (B.13) may be described by $I = [B + jC]$, where B is

$$B = \sqrt{\frac{\pi}{2}} \left(e^{-\Delta^2/2} \mp \sqrt{1 - e^{-\alpha^2}} \right) - \sum_{k=2}^{\infty} \left[\frac{(j\Delta)^k}{k!} \right] U_k \quad (k \text{ even}), \tag{B.14}$$

and

$$C = \pm \sqrt{\frac{\pi}{2}} e^{-\Delta^2/2} \left(\sqrt{e^{\Delta^2} - 1} \right) - \Delta \left(1 - e^{-\alpha^2/2} \right) - \sum_{k=2}^{\infty} \left[\frac{(j\Delta)^k}{k!} \right] U_k \quad (k \text{ odd}). \tag{B.15}$$

The signs $\mp$ and $\pm$ are determined by the signs of α and Δ, respectively. If we restrict k to unity, B and C become

$$B = \sqrt{\frac{\pi}{2}} \left(e^{-\Delta^2/2} \pm \sqrt{1 - e^{-\alpha^2}} \right), \tag{B.16}$$

$$C = \pm \sqrt{\frac{\pi}{2}} e^{-\Delta^2/2} \left(\sqrt{e^{\Delta^2} - 1} \right) - \Delta \left(1 - e^{-\alpha^2/2} \right). \tag{B.17}$$

References

[1] J. Lardies, S. Gouttebroze, Identification of modal parameters using the wavelet transform, International Journal of Mechanical Sciences (2002) 2263–2283.

[2] T.P. Le, P. Argoul, Continuous wavelet transform for modal identification using free decay response, Journal of Sound and Vibration 227 (2004) 73–100.

[3] M. Haase, J. Widjajakusuma, Damage identification based on ridges and maxima lines of the wavelet transform, International Journal of Engineering Sciences 41 (2003) 1423–1443.

[4] H. Serrai, L. Senhadji, J.D. De Certaines, J.L. Coartrieux, Time-domain quantification of amplitude, chemical shift, apparent relaxation time, and phase by wavelet-transform analysis, Application to biomedical magnetic resonance spectroscopy, Journal of Magnetic Resonances 124 (1997) 20–34.

[5] S. Qian, D. Chen, Joint Time-Frequency Analysis: Method and Application, Prentice Hall, 1996.

[6] P. Flandrin, Time-frequency and Time-scale Analysis, Academic Press, 1999.
[7] L. Cohen, Time Frequency Analysis, Prentice Hall, 1995.
[8] F. Hlawatch, G.F. Boudreaux, Linear and quadratic time-frequency signal processing, IEEE Signal Processing Magazine 9 (2) (1992) 21–67.
[9] M.H. Richardson, Global frequency and damping estimates from frequency response method, 4th IMEC conference, LA, 1986.